



# *In silico* Investigation of *Tridax procumbens* Phyto-Constituents Against SARS-CoV-2 Infection

Archana Sharbidre <sup>1,\*</sup> , Prajakta Dhage <sup>2</sup>, Harleen Duggal <sup>3</sup>, Rohan Meshram <sup>3,\*</sup> 

<sup>1</sup> Department of Zoology, Savitribai Phule Pune University, Pune 411007, MS, India

<sup>2</sup> Department of Zoology, KTHM College, Nashik- 422002, MS, India

<sup>3</sup> Bioinformatics Centre, Savitribai Phule Pune University, Pune- 411007, MS, India

\* Correspondence: aasharbidre@gmail.com (A.S.); rohan\_meshram@rediffmail.com (R.M.);

Scopus Author ID 55098329200 (R.M.)

Received: 16.11.2020; Revised: 27.12.2020; Accepted: 30.12.2020; Published: 2.01.2021

**Abstract:** *Tridax procumbens* is a popular medicinal plant traditionally used for wound healing and bronchial catarrh. In the current study, *in silico* computational analysis of 22 active phytoconstituents of *T. procumbens* was performed against SARS-CoV-2. Molecular Docking studies against six key targets of SARS-CoV-2 including PDB ID: 6LU7, a main protease 3CLpro/Mpro; PDB ID: 6NUR, SARS-Coronavirus NSP12 polymerase bound to NSP7 and NSP8 co-factors, PDB ID: 6m71, SARS-Cov-2 RNA-dependent RNA polymerase (RdRp), PDB ID: 6CS2, SARS Spike Glycoprotein - human ACE2 complex a Stabilized variant; PDB ID: 6VXX, spike glycoprotein of SARS-CoV-2 and its receptor Angiotensin-converting enzyme-2 (PDB ID: 1R42) were accomplished. Additionally, *in silico* prediction studies using pharmacokinetics (ADMET) properties and the protection profile to identify the paramount drug candidates were also done using online SwissADME and pkCSM web servers. Comprehensive docking analyses confirmed that out of 22 screened phytoconstituents, 6 compounds: Bergenin, beta-Sitosterol, Centaurein, Procumbentin, Luteolin, and Puerarin showed a high binding affinity with studied SARS-CoV-2 target proteins. Pharmacokinetics prediction studies further verified that all selected phytoconstituents were safe with good quality ADMET properties and lacking carcinogenic and tumorigenic properties. Thus, these selected drugs can effectively control COVID-19 and improve immunity, which can be confirmed by further studies.

**Keywords:** SARS-CoV-2; *Tridax procumbens*; molecular docking; ADMET analysis.

© 2020 by the authors. This article is an open-access article distributed under the terms and conditions of the Creative Commons Attribution (CC BY) license (<https://creativecommons.org/licenses/by/4.0/>).

## 1. Introduction

At the end of December 2019, a novel strain of coronavirus was detected in Wuhan city of China. It caused a pneumonia-like epidemic and is titled Severe Acute Respiratory Syndrome Coronavirus 2 (SARS-CoV-2) [1]. World Health Organization (WHO) on 11<sup>th</sup> March, 2020, announced this coronavirus disease (Covid-19) as a global pandemic in three months of its first case appearance [2-3]. Afterward, Covid-19 disease has been outspread to 216 countries encompassing India and allied zones, causing over 14, 731, 563 established cases and over 611,284 deaths as of July 22, 2020 (<https://www.who.int/emergencies/diseases/novel-coronavirus-2019>). COVID-19 sufferers show common symptoms like cold, flu, fever, and similar associated signs like sore throat, coughing, etc. However, in severe infection, it leads to acute respiratory distress syndrome (ARDS) with rarely collapsing vital organ functions,, including kidney failure, thus ultimately leading to death [4].

Even though all-inclusive efforts are being taken to cure the pandemic, clinically-proven prophylaxis, and therapeutic strategy are still demanding [5]. For active management

of COVID-19, numerous drugs have been tried or repurposed and designed predominantly targeting the host cells or immune system and directly inhibiting SARS-CoV-2 [6]. Hitherto from clinical interventions tried worldwide, to date, no medicine is available that has the ability to cure the COVID-19 completely.

Hence, in the current pandemic condition, investigation of novel bioactive compounds having a strong potential of fighting against SARS-CoV-2 viral infection is crucially essential. These compounds should also offer immunity and reinforce us to overcome this infection. Indian medicinal plants are well known for developing drugs to cure various diseases and strengthen our immune system. Besides this, the hopeful part of plant-based drugs is that they reveal less or no side effects due to their structure, which strongly reacts with pathogens and/or their toxins in such a manner that can cause the least damage to host's important bio-molecules or physiology. Throughout the COVID-19 pandemic, consumption of immuno-modulatory supplements is essential to sustain our immune system to combat the SARS-CoV-2 infection. This is also specified by India's Ministry of AYUSH by the statement, "Ayurveda's immunity-boosting measures for self-care during COVID-19 crisis" [7].

*Tridax procumbens* (Jayanti Veda) is a common, widespread weed commonly known as coat buttons plant found throughout India and a famous ethno-botanical, Ayurvedic, and Unani medicinal plant. *T. procumbens* extracts showed the existence of alkaloids, carotenoids, flavonoids (especially catechins and flavones), saponins, tannins, flavonoids (centaureidin and centaurein) and bergenin [8], lipid components like luteolin, glucoluteolin, quercetin, isoquercetin, and fumaric acid [9]. It is also an abundant source of minerals like iron, copper, manganese, sodium, and zinc [10] and other trace minerals such as magnesium, phosphorous, potassium, selenium, and calcium [11].

Its leaves are traditionally used for diabetic and non-diabetic wound healing [12-15] and procoagulant activity [16]. Its drink is also used to cure bronchial catarrh, diarrhea, dysentery [17]. Its extract possess antihyperuricemia, antioxidant, and antibacterial [18-19], antifungal [20], anti-leshmanial [21], antibiotic against challenging multidrug-resistant urinary tract bacterial isolates [22], anti-hyperglycemic [23], anti-diabetic [24], hepato-protective [25], hypotensive [26], vasorelaxant [27], immuno-modulatory [28], anti-arthritis [29], analgesic [30], anti-osteoporosis [31], anti-inflammatory [32] and anti-tubercular activity [33], and antitumor activities [34]. It is also used to cure asthma [35] and possesses antiviral activities [36-37].

So, the current study is aimed to reconnoiter the medicinal prospective of *Tridax procumbens* bioactive constituents against various proteins of SARS-CoV-2 by implementing computational methodologies. The data engendered is very promising and recommends that *Tridaxprocumbens* indeed has the competency to treat the SARS-CoV-2 infection effectively.

## 2. Materials and Methods

### 2.1. Protein retrieval and preparation.

Six fundamental targets: PDB ID: 6LU7 a main protease 3CLpro/Mpro; PDB ID: 6m71 SARS-Cov-2 RNA-dependent RNA polymerase (RdRp); PDB ID: 6NUR a recently identified SARS-Coronavirus NSP12 polymerase bound to NSP7 and NSP8 co-factors; PDB ID: 6CS2, SARS Spike Glycoprotein - human ACE2 complex a Stabilized variant; PDB ID: 6VXX, spike glycoprotein of SARS-CoV-2 and its receptor Angiotensin-converting enzyme-2 (PDB ID:

1R42) were selected for the current study. The structures were obtained from the <https://www.rcsb.org/> website in PDB format. Further, the 3D PDB file of these proteins as processed using 'A' chain and eliminating allied ligands along with crystallographic water molecules, and adding polar hydrogen atoms.

#### 2.1.1. Positive control.

Four known FDA drugs Chloroquine (CQ), Hydroxychloroquine (HCQ), Remdesivir (RDV), and Favipiravir, were selected as positive controls for the execution of blind docking. Their structures were also acquired in PDB format from the <https://www.rcsb.org/> website.

#### 2.1.2. Ligand structure preparation.

In total 22 activephyto-constituents of *T. procumbens* [38] were selected as dynamic inhibitory ligands for the existent study (details of compounds are illustrated in Supplementary Table S1. All selected ligand structures except Procumbentin were attained in SDF format from the <https://pubchem.ncbi.nlm.nih.gov/website> and changed to PDB format using Online SMILES translator and structure file generator tool [39]. Procumbentin .MOL file was generated from ChemSpiderweb tool and converted to smiles.txt file and PDB file using website: <https://cactus.nci.nih.gov/translate/>. The 2D structures were retrieved from the ChemSpider: an online chemical information resource website. [40]. The particulars of PubChem CID, molecular formulae, and 2D structures are displayed in Supplementary Table S1.

#### 2.2. Molecular docking.

First, PDB files of all selected molecules were changed in the .PDBQT format using PyRx software [41] and saved for further examination. The macromolecules, as well as ligands, were primed, and minimization of the energy was achieved. The grid box size was set at 40 X 40 X 40 the X, Y, and Z coordinates; the conf file was created using the details of PDBQT files name and grid box properties. Then by using the receptor.PDBQT file, ligand.PDBQT file and the X, Y, and Z coordinates; the binding affinity was calculated using AutoDock–Vina [42]. The best pose with the lowest binding affinity was mined for each selected ligand and positive controls. The visualization of the 3D structure of the receptor-ligand interactions together with the 2D structure of the molecular interactions was done using the Biovia Discovery Studio20.1.0 [43].

#### 2.3. Physiochemical, pharmacokinetic, and ADMET properties of *Tridaxprocumbens* phyto-constituents.

Drug-likeness properties were acquired using the SWISSADME prediction tool <http://www.swissadme.ch/>) [44]. Toxicity assessment of Phyto-constituents was achieved using the pkCSM online tool [45]. The prediction of probable side-effects or cross-reactivity of phytoconstituents was made using the Swiss target prediction web tool available with [http://www.swisstargetprediction.ch\\_website](http://www.swisstargetprediction.ch_website) [46].

### 3. Results and Discussion

The available literature was used to identify 22 active phytoconstituents of *T. procumbens*. These phytoconstituents were prepared for docking and then used for *in silico* screening against six proteins of SARS-CoV-2. Based on the Molecular docking score, the six best ligands were selected. The docking scores of all the phytoconstituents are given in Table 1.

**Table 1.** Docking results in the form of Binding Affinity of different phyto-constituents of *Tridax procumbens* used for *in silico* screening against various proteins of SARS-CoV-2 (AutoDock Vina scores are in kcal/mol).

Sr. No	Name of Compound	Docking score of <i>Tridax procumbens</i> phyto-constituents (kcal/mol) (Distance from Best Mode: 0.000 for both RMSD Lower Bound and RMSD Upper Bound)					
		6LU7	6M71	6NUR	6CS2	6VXX	1R42
01	5(alpha)- cholestane	-5.9	-5.7	-6.5	-6.8	-6.8	-8
02	alpha-Selinene	-6.3	-5.8	-6	-5.4	-6.5	-6.6
03	Bergenin	-6.4	-6.7	-7.5	-8.1	-6.4	-7
04	beta-Amyrenone	-6.5	-7.9	-8.1	-7.5	-7.3	-8.1
05	beta-Sitosterol	-6.4	-7.2	-7.9	-6.7	-7.3	-10.6
06	Betulinic acid	-5.7	-7.2	-7.4	-6.9	-6.9	-8.6
07	Caryophyllene	-6.2	-5.7	-5.9	-5.1	-5.7	-6.3
08	Centaureidin	-6.2	-7.5	-7.4	-6.8	-7.5	-6.9
09	Centaurein	-5.9	-9	-8	-6.4	-7	-8.3
10	(3,S)-16,17-Didehydrofalcarinol	-4.9	-5.1	-5.8	-4.5	-5.2	-5
11	Esculetin	-5.9	-6	-6.4	-6.6	-6.3	-6.6
12	Falcarinol	-4.6	-5.6	-5.5	-5	-4.5	-4.8
13	Limonene	-4.9	-4.9	-5.7	-5.1	-5.3	-5.7
14	Lupeol	-6	-7.6	-7.6	-7.4	-6.9	-8.3
15	Luteolin	-7	-7.6	-8.5	-7.4	-7.1	-7.8
16	Methyl 10-oxooctadecanoate	-4.4	-4.3	-4.5	-4.2	-5.1	-5.3
17	Procumbentin	-6.4	-8.5	-8.7	-7.6	-6.7	-8.7
18	Puerarin	-6.7	-7.8	-7.9	-6.7	-8.2	-8
19	Stigmasterol	-6.6	-7.4	-8.3	-7	-7	-8.3
20	Taraxasterol acetate	-6.3	-8	-7.8	-6.5	-7.2	-8.5
21	Voacangine	-5.8	-7.1	-7.4	-6.1	-6.1	-7.1
22	Zerumbone	-6.4	-5.9	-6.1	-5.5	-5.6	-6.4
Positive controls							
1	Chloroquine	-5.3	-5.4	-6.2	-5.8	-5.6	-6.8
2	Favipiravir	-5.7	-5.3	-5.7	-5.7	-5	-5.5
3	Hydroxychloroquine	-5.6	-5.7	-6	-5.5	-5.9	-6.4
4	Remdesivir	-5.5	-6.5	-8.1	-6	-6	-6.6

#### 3.1. The binding affinity of selected compounds.

Among the 22 phytoconstituents screened (Table 1), the binding energies for about 9 compounds were lesser than the upper threshold (-6 kcal/mol), generally considered as a cut-off in ligand-binding studies, but we also observed that 5 of these compounds were very close to this threshold.

Table 1 shows the binding affinity of all 22 phytoconstituents toward six proteins of SARS-CoV-2 screened in this study. Table 1 also displays variation in binding energy amongst each ligand and various SARS-CoV-2 macromolecules tested. The frequency distribution

range of obtained Docking scores (kcal/mol) of various phytoconstituents of *T. procumbens* against various proteins of SARS-CoV-2 is illustrated in Figure 1. Table 2 shows the six topmost ligands showing the highest docking score are listed based on binding energy.

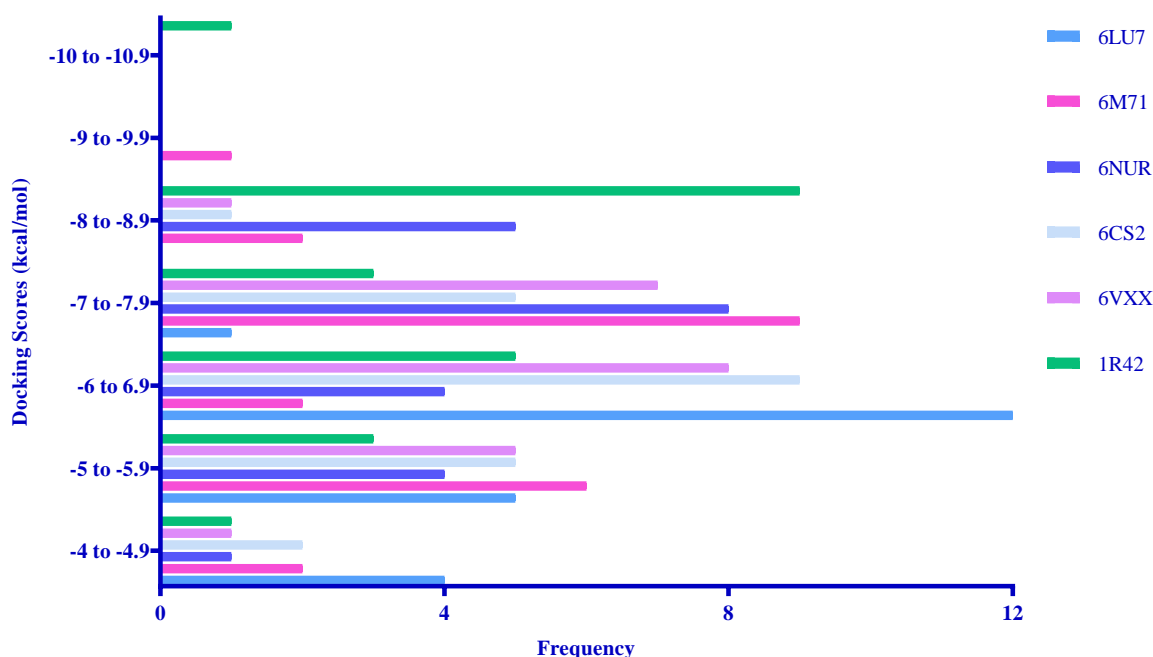


**Figure 1.** Frequency distribution of Docking scores (kcal/mol) range of various phytoconstituents of *Tridax procumbens* used for *in silico* screening against various proteins of SARS-CoV-2.

**Table 2.** Six Topmost compounds with the highest binding energy selected using docking results arranged as per their binding affinity score.

Sr. No	Name of Selected ligand	Interaction with SARS-CoV-2 protein	Docking score (kcal/mol)	Interacting Residues
1.	beta-Sitosterol (PubChem CID-222284 )	1R42	-10.6	PRO346 <sup>a</sup> , PHE390 <sup>d</sup> , ARG393 <sup>d</sup> , PHE40 <sup>d</sup> , ALA348 <sup>d</sup> , HIS378 <sup>d</sup>
2.	Centaurein (PubChem CID-5489090 )	6M71	-9	GLU811 <sup>a</sup> , SER814 <sup>a</sup> , LYS798 <sup>a</sup> , LYS621 <sup>c</sup> , PRO620 <sup>c</sup> , TRP617 <sup>c</sup> , TRP800 <sup>c</sup> , ASP761 <sup>b</sup> , PRO620 <sup>d</sup> , LYS798 <sup>d</sup>
3.	Procumbentin	6NUR	-8.7	ARG249 <sup>a</sup> , LEU251 <sup>a</sup> , ARG349 <sup>a</sup> , THR246 <sup>b</sup> , THR319 <sup>b</sup> , LEU245 <sup>c</sup> , PRO323 <sup>c</sup> , PRO677 <sup>c</sup> , PHE396 <sup>c</sup> , VAL675 <sup>c</sup> , PRO461 <sup>d</sup> , ARG249 <sup>d</sup>
4.	Puerarin (PubChem CID-5281807 )	6VXX	-8.2	ASN317 <sup>a</sup> , SER316 <sup>a</sup> , TYR612 <sup>c</sup> , VAL595 <sup>c</sup> , PHE318 <sup>c</sup> , LYS304 <sup>c</sup> , THR302 <sup>c</sup> , ALA292 <sup>d</sup> , CYS291 <sup>d</sup> , CYS301 <sup>d</sup> , GLU298 <sup>d</sup>
5.	Bergenin (PubChem CID-66065 )	6CS2	-8.1	LEU843 <sup>a</sup> , ASP757 <sup>a</sup> , LYS715 <sup>a</sup> , ASP849 <sup>b</sup> , PRO1039 <sup>b</sup> , HIS1040 <sup>b</sup> , PRO845 <sup>d</sup>
6.	Luteolin (PubChem CID-5280445)	6LU7	-7	ARG105 <sup>a</sup> , ILE152 <sup>a</sup> , GLN110 <sup>a</sup> , THR111 <sup>a</sup> , GLN107 <sup>c</sup> , ILE106 <sup>c</sup> , PHE294 <sup>d</sup> , VAL104 <sup>d</sup> , ASP153 <sup>c</sup> , PHE8 <sup>c</sup> , ASN151 <sup>c</sup> , THR292 <sup>c</sup>

a-Hydrogen bond; b-Carbon Hydrogen bond; c-van der Waals; d-Hydrophobic interactions

The binding affinity for COVID-19 6LU7, a main protease 3CLpro/Mpro was in the range -4.4 kcal/mol (for Methyl 10-oxooctadecanoate) to -7 kcal/mol (for Luteolin). Overall, the lowest binding scores for all ligands were observed against this macromolecule. The

binding affinity for COVID-19 6m71 RdRp was in the range -4.3 kcal/mol (for Methyl 10-oxooctadecanoate) to -9 kcal/mol (for Centaurein). The binding affinity for COVID-19 6NUR SARS-Coronavirus NSP12 polymerase was in the range -4.5 kcal/mol (Methyl 10-oxooctadecanoate) to -8.7 kcal/mol (for Procumbentin). The binding affinity for COVID-19 6CS2, SARS Spike Glycoprotein - human ACE2 complex was in the range -4.2 kcal/mol (for Methyl 10-oxooctadecanoate) to -8.1 kcal/mol (for Bergenin). The lowest binding score was observed for this macromolecule compared to the other five with all ligand docking scores. The binding affinity range for COVID-19 6VXX, spike glycoprotein of SARS-CoV-2 was from -4.5 kcal/mol (for Methyl 10-oxooctadecanoate) to -8.2 kcal/mol (for Puerarin), and for spike glycoprotein receptor Angiotensin-converting enzyme-2, 1R42 ranged between -4.8 kcal/mol (for Methyl 10-oxooctadecanoate) and -10.6 kcal/mol for beta-Sitosterol which is the highest docking score obtained from all ligands.

Thus we can clearly say that the ligand Methyl 10-oxooctadecanoate showed the lowest binding affinity against all receptors tested, whereas Procumbentin showed the highest binding affinity for maximum receptors (four) amongst all ligands screened herewith.

Interestingly the known antiviral drugs tested show binding scores in the range of -5 to -8.1 kcal/mol, which is far less than the score obtained for the majority of *T. procumbens* phytoconstituents. So we can confidently and intensely state that these phytoconstituents have much superior COVID-19 receptor inhibition capacity tested herein than these well-known approved drugs used as a positive control.

For convenience, the best 6 phyto-constituents of *T. procumbens* who showed noticeable results against all six receptors checked were selected for further analysis and compared with Remdesivir. It showed an overall good docking score (Table 1).

The interaction between SARS-CoV-2 amino acid residues with these selected phytoconstituents is displayed in Table 2. These phytoconstituents have validated commendable free energy of binding interactions with SARS-CoV-2 proteins (Table 2). The possible binding orientation of these selected phytoconstituents within SARS-CoV-2 proteins, along with conforming hydrogen bonds and hydrophobic interactions, are correspondingly exemplified in Table 2.

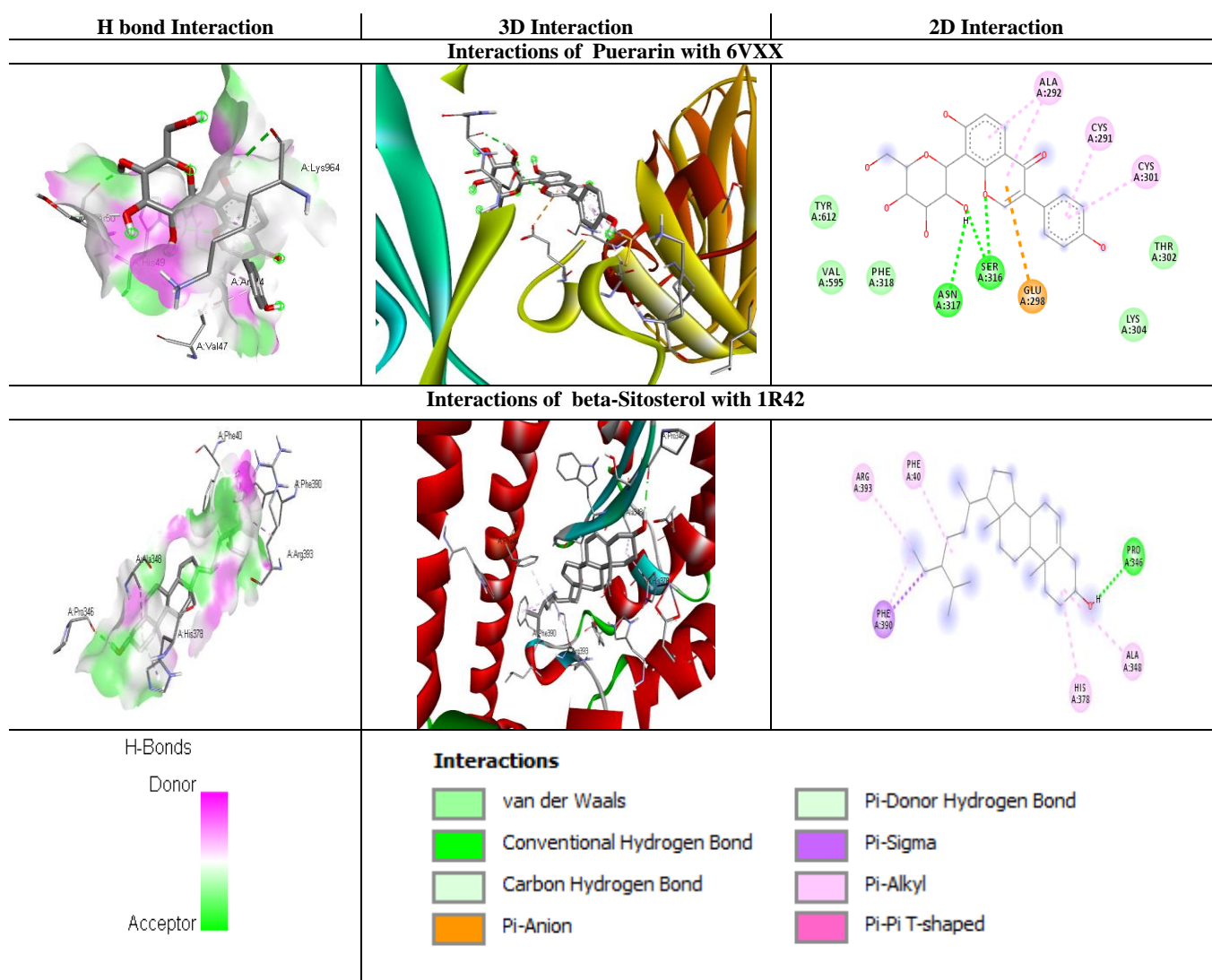
The binding orientation of these top 6 phyto-constituents with each with receptor was studied using Discovery studio visualizer, and best poses in 2D and 3D were produced (Table 3). Furthermore, comprehensive docking analyses demonstrated that beta-Sitosterol, Centaurein, and Procumbentin show a high binding affinity with the studied target proteins SARS-CoV2 followed by others, and the highest binding affinity was displayed by beta-Sitosterol.

### 3.2. Prediction of pharmacokinetic and ADMET properties.

Lipinski's rule of 5 is treated as a great method for assessing drug likeliness, which helps discover whether a specific chemical compound has certain biological and physiochemical properties that would succeed as a feasible orally active drug in humans. Lipinski's rule guesses five assorted properties imperative for drug designing. Lipinski's rule of five states that (i) molecular mass less than 500 Daltons, (ii) no more than 5 H-bond donors, (iii) no more than 10 H-bond acceptors, (iv) O/W partition coefficient log P not greater than 5. Suppose the molecule violates more than 3 descriptor constraints. In that case, it will not fit into the drug likeliness standards, and it is not considered for drug discovery [47]. A standard TPSA clarifies that the ligand has copious transport properties.







From the data obtained, we can say that most of the compounds tried to follow the rules, and some of them not. Nearly all compounds showed good synthetic accessibility value suggesting all the phytoconstituents can be synthesized. Overall results strongly agree that active phyto-components of *T. procumbens* retain drug-likeness properties.

The pharmacokinetics properties and predicted ADMET properties of *T. procumbens* phytoconstituents were calculated using the pkCSM web tool. From the attained data, we can conclude that all studied compounds have the utmost gastro-intestinal absorption (> 85 %), human tissue distribution (VDss), and entire abundant clearance (Supplementary Table. S4). Betulinic acid and Taraxasterol acetate possess maximum bioavailability (> 98 %). In the Metabolism Properties, the Cytochrome P450 and P-glycoprotein simulation method for both substrate and inhibition was done for all *T. procumbens* phytoconstituents pkCSM web tool. The results indicate that most of them have lower CYP inducing and P-gp compatibility properties (Supplementary Table. S4). The toxicity assessment test revealed that only a few compounds have deviated from toxicity prediction. Overall, the study specifies that most *T. procumbens* phytoconstituents are devoid of carcinogenic, teratogenic, and tumorigenic properties (Supplementary Table. S4).

The details of Physiochemical and ADMET properties of 6 selected *T. procumbens* phytoconstituents are further presented in Table 4. The PSA is closely linked to the absorption properties of compounds. Except for Luteolin and Bergenin, the other five phytoconstituents' PSA was greater than 140, signifying that these compounds had strong polarity and thus not



easily absorbed by the body. Luteolin and Bergenin showed good oral absorption or membrane permeability [48]. Except for beta-Sitosterol(LogP> 5) [49], all others were predicted as having the best lipophilicity (LogP ≤ 5).

The predicted Absorption properties include proCaco-2 permeability, intestinal absorption (human), skin permeability, and P-glycoprotein substrate or inhibitor. Only beta-Sitosterol showed the predicted value >0.90 showing high Caco-2 permeability and maximum absorption. Concerning intestinal absorption (human), the absorbance of less than 30% is measured to be poorly absorbed. All six selected compounds showed higher than this threshold, indicating good predicted absorption. For skin permeability, the log Kp>2.5 is reflected as low skin permeability. All six selected phytoconstituents showed high skin permeability. P-glycoprotein results recommended that all compounds are substrates of P-glycoprotein except for beta-Sitosterol and predicted to be actively released from cells by P-glycoprotein. beta-Sitosterol was predicted to be a P-glycoprotein inhibitor.

The distribution volume (VDss), Fraction unbound (human), CNS permeability, and blood-brain barrier membrane permeability (logBB) characterize the distribution of compounds. Procumbentin, Bergenin, and Luteolin high distribution volume (log VDss> 0.45). Except for beta-Sitosterol, all other selected phytoconstituents were non-permeable for blood-brain barrier membrane (logBB< -1). Only beta-Sitosterol and Luteolin were predicted to penetrate the CNS (logPS> -2). As Cytochrome P450s (CYP) is a vital enzyme system for drug metabolism in the liver, the results showed that excluding beta-Sitosterol, all other selected phytoconstituents were not substrates for CYP3A4. All selected compounds are CYP inhibitors proposing that they could be metabolized in the liver.

**Table 4.** Predicted ADMET properties of six selected phytoconstituents of *T. procumbens*.

Properties	beta-Sitosterol	Centaurein	Procumbentin	Luteolin	Bergenin	Puerarin
Polar Surface Area (PSA)	187.039	208.748	206.858	117.313	129.813	169.199
LogP	8.0248	0.0757	-0.5217	2.2824	-1.2006	0.3861
Synthetic accessibility	6.30	5.70	5.69	3.02	4.39	4.98
Water solubility (log mol/L)	-6.773	-2.995	-2.918	-3.094	-1.853	-2.72
Caco2 per. (log Papp in 10 <sup>-6</sup> cm/s)	1.201	0.294	-1.418	0.096	0.289	0.223
Intestinal ab (human) (% Absorbed)	94.464	35.872	31.97	81.13	63.774	67.446
Skin Permeability (log Kp)	-2.783	-2.735	-2.735	-2.735	-2.736	-2.735
P-gp substrate	No	Yes	Yes	Yes	Yes	Yes
P-gp I inhibitor	Yes	No	No	No	No	No
P-gp II inhibitor	Yes	No	No	No	No	No
VDss (human) (log L/kg)	0.193	0.211	1.132	1.153	0.68	0.377
Fraction unbound (human) (Fu)	0	0.114	0.143	0.168	0.632	0.187
BBB permeability (log BB)	0.781	-1.976	-2.407	-0.907	-1.091	-1.204
CNS permeability(log PS)	-1.705	-4.267	-4.826	-2.251	-3.903	-3.594
(log ml/min/kg)	No	No	No	No	No	No
CYP3A4 substrate	Yes	No	No	No	No	No
CYP1A2 inhibitor	No	No	No	Yes	No	No
CYP2C19 inhibitor	No	No	No	No	No	No
CYP2C9 inhibitor	No	No	No	Yes	No	No
CYP2D6 inhibitor	No	No	No	No	No	No
CYP3A4 inhibitor	No	No	No	No	No	No

Properties	beta-Sitosterol	Centaurein	Procumbentin	Luteolin	Bergenin	Puerarin
Total Clearance (log ml/min/kg)	0.628	0.536	0.429	0.495	0.427	-0.007
Renal OCT2 substrate	No	No	No	No	No	No
AMES toxicity	No	No	No	No	No	No
MTD @ (log mg/kg/day)	-0.621	0.56	0.531	0.499	-0.013	0.642
hERG I inhibitor	No	No	No	No	No	No
hERG II inhibitor	Yes	Yes	Yes	No	No	Yes
ORT* (mol/kg)	2.552	2.565	2.574	2.455	1.879	2.641
ORCT# (log mg/kg_bw/day)	0.855	3.805	4.089	2.409	3.614	4.85
HEP\$	No	No	No	No	No	No
SS^	No	No	No	No	No	No
TPT+ (log ug/L)	0.43	0.285	0.285	0.326	0.285	0.285
Minnow toxicity (log mM)	-1.802	6.387	7.199	3.169	5.688	4.188

Synthetic accessibility range (0-10) = very easy to very difficult to synthesize; \*P-gp- P -glycoprotein; @MTD-Max. tolerated dose (human);\*ORT-Oral Rat Acute Toxicity (LD50) ; #ORCT- Oral Rat Chronic Toxicity (LOAEL) ; HEP\$-Hepatotoxicity; ^SS-Skin Sensitisation; +TPT-T.Pyriformis toxicity

**Color codes:** Dark Orange for highly positive (Yes); Orange for weak positive (Moderate); Light green for negative (No).

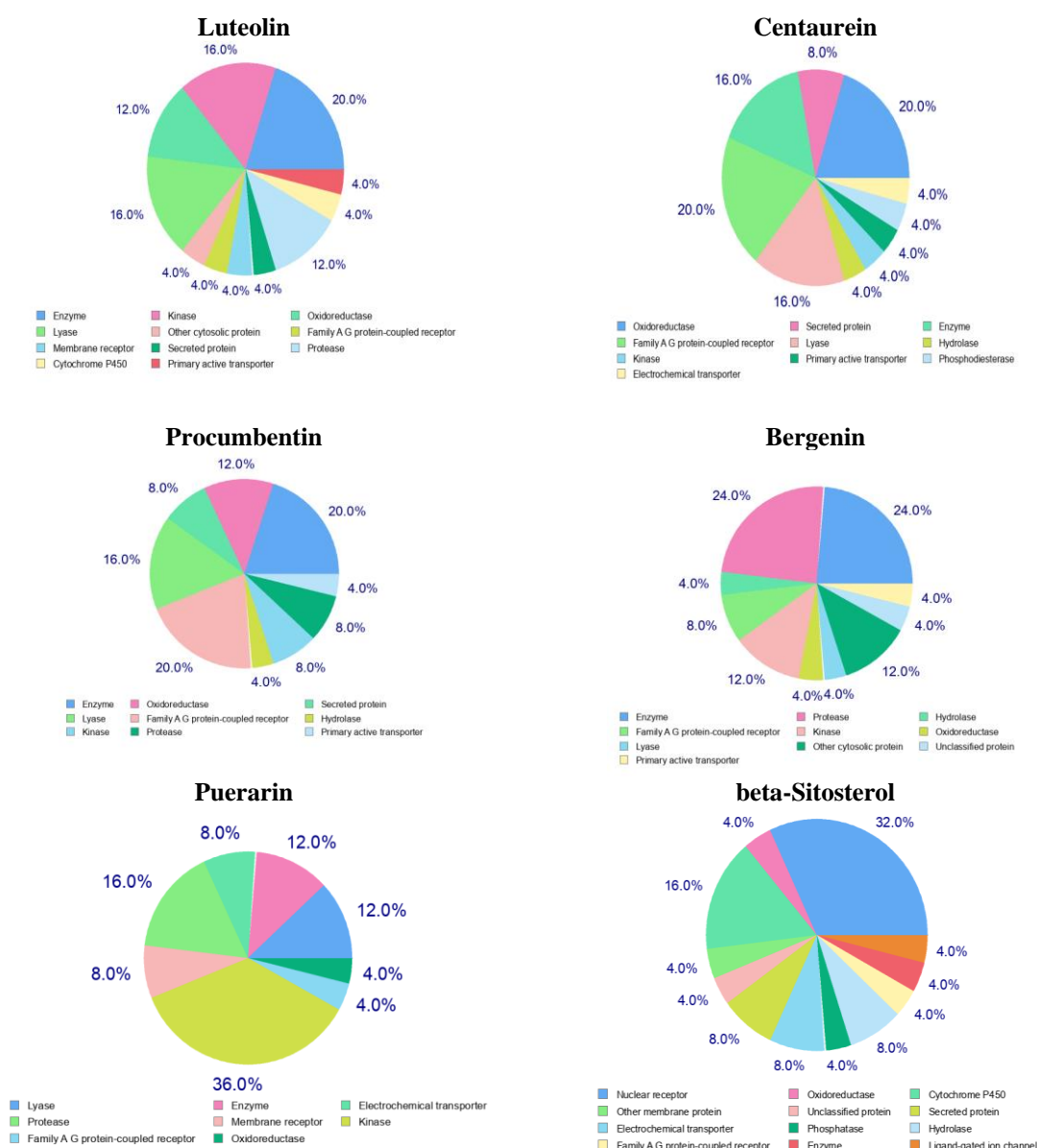


**Figure 2.** Top 25 of Target Predicted for six selected phytoconstituents of *T. procumbens* used for *in silico* screening against various proteins of SARS-CoV-2.

Excretion of Drug is dependent on its molecular weight and hydrophilicity. Excretion's prediction results demonstrated that all selected compounds' total clearance is the higher; they are non-toxic in the AMES test; non-hepatotoxic, but may not inhibit the hERG channel not induce cardiotoxicity or skin sensitization.

Six best-selected compounds were further screened for target prediction analysis using the SwissTargetPrediction web tool [50]. The top 25 interpretations are shown in the pie chart format in Figure 2. The pie chart predicts % of various enzymes and receptors.

Thus, the predicted outcomes specify that the ADMET characteristics of most of the selected compounds are safe for humans.

### 3.3. Discussion.

In modern drug discovery, computer-aided drug design (CADD) has turned out to be a vibrant program as it not only considerably curtails the cost and labor involved in the drug discovery process but also speeds it up by allowing the scientists to limit their efforts during biological and synthetic testing [51]. Besides molecular docking, numerous ADMET tools are also available and are equally considered as an important constituent in the CADD due to their trustworthy predictions [52]. The compounds succeeding the Druglikeness tests without violating rules confirm their efficacy as a good drug in the biological systems and allow them for further biochemical analysis. In contrast, toxicity prediction approves its safety for human consumption [53].

The illustrious fact of modern drugs is to kill the virus without improving the host immunity customarily. In this concern, the phytoconstituents of *T. procumbens* were selected for the current study. As mentioned earlier, *T. procumbens* drink is traditionally used to treat bronchial catarrh [17] and asthma [35]. It also possesses antiviral [37], immunomodulatory [28], anti-inflammatory [32] and analgesic [30] properties.

The present study results highlighted that out of 22 selected phytoconstituents, 18 compounds showed good binding affinity. Compounds like beta-Amyrenone, Betulinic acid, Lupeol, Stigmasterol, Taraxasterol acetate, and Voacangine exhibited overall high binding affinity towards most targets selected. Likewise, they are also found to be vital drugs as they all have excellent synthetic accessibility.

Figure 2 represents the percentage of these six selected phytoconstituents to target various enzymes with different activities. Some of which have been mentioned in previously published studies.

In the current study, six compounds showed the highest antiviral activity against six proteins of SARS-CoV-2. These top six selected ligands, including beta-Sitosterol, is a proven potential antioxidant [54]; anti-inflammatory compound with the least toxicity and insignificant ulcerogenic activities [55]. The Interaction analysis was performed for each of the complex and was compared to other studies to infer the residue wise contribution in the activity. Angiotensin-Converting Enzyme-Related Carboxypeptidase has been proposed as a suitable target in different studies using in-vitro techniques [56]. Pro346, His 378 are conserved residues of the catalytic motif indicating interactions with these residues to be crucial for the Enzyme-Inhibitor complex's stability. Also, His378 is one of the residues that are conserved among sACE and tACE enzymes [57]. The carbonyl oxygen of Pro346 forms a hydrogen bond with the secondary amine of its known inhibitor MLN4760 [57].

6M71: The polymerase activity of RNA-dependent RNA polymerase is performed by forming a conserved arch which includes three subdomains Finger subdomain (Lys621), Palm

subdomain (His811, Ser814, Pro620, Trp617, Asp761, Lys 798, Trp800), and Thumb subdomain [58]. The interaction with these residues contributes to the polymerase activity of the enzyme. Centaurin strongly binds within the enzyme's active site (Table 2) by forming interactions with these residues. ASP761, LYS798, and Ser814 interact with the ligand while the other residues create an interface for the enzyme-ligand complex to interact. [59]. Lys 798 stabilizes the core domain of the enzyme while the interaction with Asp761 creates a catalytic domain, and Ser814 positions the nucleotides, which is in-line with the previously published research articles. [60-62]. The antiviral activity of Centurion has been previously studied [63].

6LU7: The main protease has been identified as a possible target. It plays a crucial role in the SARS virus's pathogenesis. Covalent interactions with Gln110 plays a vital role in the formation of the substrate-enzyme complex [64]. In previously published studies, a point mutation Thr292Ala shows an enzyme's enhanced activity [65]. Thr292 helps approach the domain III of the dimer more closely, due to which the hydrophobic backbone of the residues form a bed for the catalytic activity of the enzyme. Luteolin has been identified to inhibit the virus by anticomplementary activity [65-66]. Besides Mpro, Luteolin has shown inhibition against GST-S2, 3CLpro, Serine protease [66-68].

6CS2: The spike protein residues Asp757 and Asp849 play a crucial role in the viral entry [69]. Proline residues restrain the bend conformation, which is favorable for the active site's interaction with the residue and constrain the flexible conformation as it has the highest turn induction propensity [70]. Leu843 contributes to a major antigenic determinant of SARS-COV Spike protein that helps neutralize antibodies. Also, the leucine zipper has been characterized as a conserved motif of many viral glycoprotein families and is seen to be conserved in the S-protein of the coronavirus as well [71]. Bergenin, which showed antiviral activity against the enzyme, shows antiviral activity against Influenza and HIV as well [72-73]. The anti-inflammatory activity of Bergenin is in standard with Ibuprofen, as mentioned in the previous study [74]. Also, the anti-inflammatory activity of the potential inhibitor has shown reasonable activity against IL-6 [75].

6VXX: The Phe318 has been identified as a conserved residue in the spike glycoproteins (closed state) of the virus [76]. It has been known that the coronavirus S glycoprotein is surface-exposed and mediates entry into host cells. Hence, it can be considered as the main focus of therapeutics and vaccine development. Puerarin has been known to have anti-inflammatory effects. It functions by affecting immunocytes, signaling pathways, and cytokines [77]. The pharmacodynamic properties of Puerarin are well studied [78]. It has been identified as an alternative to hydroxychloroquine with less or no side effects [79]. Puerarin has shown good activity against the spike protein and having a good ADME toxicity profile, as shown in the study also meets Lipinski's rule to some extent [79].

6NUR: Coronavirus Nsp12 polymerase plays a crucial role in the RNA synthesis machinery of the virus [80]. The Arg249 is a subpart of the NIRAN domain, while the Leu251 is a part of the interface domain that acts as a junction and maintains interactions between the finger domain, NIRAN domain, and second subunit that together contribute to the enzyme activity [81]. Leu's presence, which is a mutation for Val, has been known to induce a better base pairing with nsp12 polymerase, excluding its analog in the active site. Arg249, Thr246, Leu245 are the residues that form the NIRAN subunit while Leu251, Thr319, Pro323, Arg349, Phe396 form the interface domain [82].

Centaurein possesses anti-inflammatory action by stimulating IFN- $\gamma$  expression [83]. Luteolin possess anti-oxidant, anti-inflammatory, anti-allergic [84] and antitumor [85]

properties. Bergenin also displays anti-malarial [86], anti-hepatotoxic, anti-HIV, hepatoprotective, anti-inflammatory with immuno-modulatory properties [87], and also potential inhibitors against the main protease of SARS-CoV-2 [88]. Puerarin exhibited antioxidant and anti-inflammatory, properties [89]. The most promising ligand found here is Procumbentin, which is known for its anti-nociceptive property [90]. In the current study, it showed a very good binding affinity against all studied macromolecules. So it would be very interesting to study it in detail in the future.

#### 4. Conclusions

In the search for a new natural drug that can inhibit SARS-CoV-2 infection and provide immunity, by using molecular docking technique and ADMET analysis, total 22 phytoconstituents of *Tridax procumbens* were screened. Six molecules among these 22 were prequalified as they are fascinating both from a chemical and biological perspective. Hence it is recommended that these six molecules can be used as an inhibitor of various proteins of SARS-CoV-2 along with anti-inflammatory with immuno-modulatory potential. Additionally, they are also non-toxic and non-carcinogenic. Thus, this study proposes that these selected phytoconstituents of *T. procumbens* can effectively control COVID-19 and modify human immunity, validated by further studies.

#### Funding

This research received no external funding.

#### Acknowledgments

This research has no acknowledgment.

#### Conflicts of Interest

The authors declare no conflict of interest.

#### References

1. Chen, N.; Zhou, M.; Dong, X.; Qu, J.; Gong, F.; Han, Y.; Qiu, Y.; Wang, J.; Liu, Y.; Wei, Y.; Xia, J.; Yu, T.; Zhang, X.; Zhang, L. Epidemiological and clinical characteristics of 99 cases of 2019 novel coronavirus pneumonia in Wuhan, China: a descriptive study. *Lancet* (London, England) **2020**, *395*, 507-513, [https://doi.org/10.1016/S0140-6736\(20\)30211-7](https://doi.org/10.1016/S0140-6736(20)30211-7).
2. Bogoch, I.I.; Watts, A.; Thomas-Bachli, A.; Huber, C.; Kraemer, M.U.; Khan, K. Pneumonia of unknown aetiology in Wuhan, China: potential for international spread via commercial air travel. *J Travel Med.* **2020**, *27*, <https://doi.org/10.1093/jtm/taaa008>.
3. Hui, D.S.; Azhar, E. I.; Madani, T. A.; Ntoumi, F.; Kock, R.; Dar, O.; Ippolito, G.; Mchugh, T.D.; Memish, Z.A.; Drosten, C.; Zumla, A. The continuing 2019-nCoV epidemic threat of novel coronaviruses to global health - The latest 2019 novel coronavirus outbreak in Wuhan, China. *Int J Infect Dis.* **2020**, *91*, 264-266, <https://doi.org/10.1016/j.ijid.2020.01.009>.
4. Huang, C.; Wang, Y.; Li, X.; Ren, L.; Zhao, J.; Hu, Y.; Zhang, L.; Fan, G.; Xu, J.; Gu, X.; Cheng, Z. Clinical features of patients infected with 2019 novel coronavirus in Wuhan, China. *Lancet* (London, England) **2020**, *395*, 497-506, [https://doi.org/10.1016/S0140-6736\(20\)30183-5](https://doi.org/10.1016/S0140-6736(20)30183-5).
5. Xu, B.; Gutierrez, B.; Mekaru, S.; Sewalk, K.; Goodwin, L.; Loskill, A.; Cohn, E.L.; Hsuen, Y.; Hill, S.C.; Cobo, M.M.; Zarebski, A.E.; Li, S.; Wu, C.H.; Hulland, E.; Morgan, J.D.; Wang, L.; O'Brien, K.; Scarpino, S.V.; Brownstein, J.S.; Pybus, O.G.; Pigott, D.M.; Kraemer, M.U.G. Epidemiological data from the COVID-19 outbreak, real-time case information. *Sci Data.* **2020**, *7*, <https://doi.org/10.1038/s41597-020-0448-0>.
6. Zhou, Y.; Hou, Y.; Shen, J.; Huang, Y.; Martin, W.; Cheng, F. Network-based drug repurposing for novel coronavirus 2019-nCoV/SARS-CoV-2. *Cell Discov.* **2020**, *6*, 1-18, <https://doi.org/10.1038/s41421-020-0153-3>.



7. Ministry of Ayush. Ayurveda's immunity boosting measures for self-care during COVID 19 crisis [WWW Document]. **2020**, <https://www.ayush.gov.in/docs/123.pdf>.
8. Jachak, S.M.; Gautam, R.; Selvam, C.; Madhan, H.; Srivastava, A.; Khan, T. Anti-inflammatory, cyclooxygenase inhibitory and antioxidant activities of standardized extracts of *Tridax procumbens* L. *Fitoterapia* **2011**, *82*, 173-177, <https://doi.org/10.1016/j.fitote.2010.08.016>.
9. Taddei, A.; Rosas-Romero, A.J. Bioactivity studies of extracts from *Tridax procumbens*. *Phytomedicine* **2000**, *7*, 235-238, [https://doi.org/10.1016/S0944-7113\(00\)80009-4](https://doi.org/10.1016/S0944-7113(00)80009-4).
10. Ikewuchi, C.C.; Ikewuchi, J.C.; Ifeanacho, M.O. Phytochemical composition of *Tridax procumbens* Linn leaves: Potential as a functional food. *Food Nutr Sci*. **2015**, *6*, <https://doi.org/10.4236/fns.2015.611103>.
11. Thalkari, A.B.; Karwa, P.N.; Shinde, P.S.; Gawli, C.S.; Chopane, P.S. Pharmacological actions of *Tridax procumbens* L.: A Scientific Review. *Res. J. Pharmacognosy and Phytochem.* **2020**, *12*, 27-30, <https://doi.org/10.5958/0975-4385.2020.00006.0>.
12. Ravindran, J.; Arumugasamy, V.; Baskaran, A. Wound healing effect of silver nanoparticles from *Tridax procumbens* leaf extracts on *Pangasius hypophthalmus*. *Wound Medicine*. **2019**, *27*, <https://doi.org/10.1016/j.wndm.2019.100170>.
13. Suryamathi, M.; Ruba, C.; Viswanathamurthi, P.; Balasubramanian, V.; Perumal, P. *Tridax procumbens* extract loaded electrospun PCL nanofibers: a novel wound dressing material. *Macromol. Res.* **2019**, *27*, 55-60, <https://doi.org/10.1007/s13233-019-7022-7>.
14. Ambulkar, S.; Ambulkar, P.; Deshmukh, M.P.; Budhrani, A.B. Experimental Evaluation of Wound Healing Activity of Various Dosage Forms of *Tridax Procumbens*. *Indian J Med Forensic Med Toxicol.* **2020**, *14*, 6579-6584, <https://doi.org/10.37506/ijfmt.v14i4.12641>.
15. Shrivastav, A.; Mishra, A.K.; Abid, M.; Ahmad, A.; Fabuzinadah, M.; Khan, N.A. Extracts of *Tridax procumbens* linn leaves causes wound healing in diabetic and Non-diabetic laboratory animals. *Wound Medicine*. **2020**, *29*, <https://doi.org/10.1016/j.wndm.2020.100185>.
16. Gubbiveeranna, V.; Kusuma, C.G.; Bhavana, S.; Sumachirayu, C.K.; Ravikumar, H.; Nagaraju, S. Potent procoagulant and platelet aggregation inducing serine protease from *Tridax procumbens* extract. *Phcog Res.* **2019**, *11*, 363-370, [https://doi.org/10.4103/pr.pr\\_4\\_19](https://doi.org/10.4103/pr.pr_4_19).
17. Ali, M.; Ravinder, E.; Ramachandram, R. A new flavonoid from the aerial parts of *Tridax procumbens*. *Fitoterapia*. **2001**, *72*, 313-315, [https://doi.org/10.1016/S0367-326X\(00\)00296-3](https://doi.org/10.1016/S0367-326X(00)00296-3).
18. Andriana, Y.; Xuan, T. D.; Quy, T. N.; Minh, T. N.; Van, T. M.; Viet, T.D. Antihyperuricemia, Antioxidant, and Antibacterial Activities of *Tridax procumbens* L. *Foods* **2019**, *8*, <https://doi.org/10.3390/foods8010021>.
19. Syed, A.; Benit, N.; Alyousef, A.A.; Alqasim, A.; Arshad, M. *In-vitro* antibacterial, antioxidant potentials and cytotoxic activity of the leaves of *Tridax procumbens*. *Saudi J Biol Sci.* **2020**, *27*, 757-761, <https://doi.org/10.1016/j.sjbs.2019.12.031>.
20. Policegoudra, R.S.; Chattopadhyay, P.; Aradhya, S.M.; Shivaswamy, R.; Singh, L.; Veer, V. Inhibitory effect of *Tridax procumbens* against human skin pathogens. *J. Herb. Med.* **2014**, *4*, 83-88, <https://doi.org/10.1016/j.hermed.2014.01.004>.
21. Gamboa-Leon, R.; Vera-Ku, M.; Peraza-Sanchez, S.R.; Ku-Chulim, C.; Horta-Baas, A.; Rosado-Vallado, M. Antileishmanial activity of a mixture of *Tridax procumbens* and *Allium sativum* in mice. *Parasite* **2014**, *21*, <https://doi.org/10.1051/parasite/2014016>.
22. Al-Ansari, M.M.; Dhasarathan, P.; Ranjitsingh, A.J.A.; Al-Humaid, L.A. Challenging multidrug-resistant urinary tract bacterial isolates via bio-inspired synthesis of silver nanoparticles using the inflorescence extracts of *Tridax procumbens*. *J. King Saud Univ. Sci.* **2020**, *32*, 3145-3152, <https://doi.org/10.1016/j.jksus.2020.08.028>.
23. Pareek, H.; Sharma, S.; Khajja, B.S.; Jain, K.; Jain, G.C. Evaluation of hypoglycemic and anti-hyperglycemic potential of *Tridax procumbens* (Linn.). *BMC Complement Altern Med.* **2009**, *9*, <https://doi.org/10.1186/1472-6882-9-48>.
24. Bhagat, V.C.; Kondawar, M.S. Antitubercular Potential of *Dendrophthoe Falcate* (L.) And *Tridax Procumbens* (L.) Plants Extracts Against H37rv Stain of Mycobacteria Tuberculosis. *Int. J. Pharm. Sci.* **2019**, *10*, 251-259, [https://doi.org/10.13040/IJPSR.0975-8232.10\(1\).251-59](https://doi.org/10.13040/IJPSR.0975-8232.10(1).251-59).
25. Ravikumar, V.; Shivashangari, K.S.; Devaki, T. Hepatoprotective activity of *Tridax procumbens* against d-galactosamine/lipopolysaccharide-induced hepatitis in rats. *J Ethnopharmacol.* **2005**, *101*, 55-60, <https://doi.org/10.1016/j.jep.2005.03.019>.
26. Salahdeen, H.M.; Yemitan, O.K.; Alada, A.R.A. Effect of aqueous leaf extract of *Tridax procumbens* on blood pressure and heart rate in rats. *Afr. J. Biomed. Res.* **2004**, *7*, <https://doi.org/10.4314/ajbr.v7i1.54062>.
27. Salahdeen, H.M.; Idowu, G.O.; Yemitan, O.K.; Murtala, B.A.; Alada, A.R. The relaxant actions of ethanolic extract of *Tridax procumbens* (Linn.) on rat corpus cavernosum smooth muscle contraction. *J Basic Clin Physiol Pharmacol.* **2015**, *26*, 211-216.
28. Oladunmoye, M.K. Immunomodulatory effects of ethanolic extract of *Tridax procumbens* on swiss Albino rats orogastrically dosed with *Pseudomonas aeruginosa* (NCIB 950). *Int. J. Trop. Med.* **2006**, *1*, 152-155, <https://dx.doi.org/10.3923/tmr.2006.122.126>.

29. Petchi, R.R.; Vijaya, C.; Parasuraman, S. Anti-arthritis activity of ethanolic extract of *Tridax procumbens* (Linn.) in Sprague Dawley rats. *Pharmacognosy Res.* **2013**, *5*, <https://dx.doi.org/10.4103%2F0974-8490.110541>.
30. Prabhu, V.V.; Nalini, G.; Chidambaramathan, N.; Kisan, S.S. Evaluation of anti-inflammatory and analgesic activity of *Tridax procumbens* Linn. against formalin, acetic acid and CFA induced pain models. *Int J Pharm Pharm Sci.* **2011**, *3*, 126-130, <https://doi.org/10.18203/2319-2003.ijbcp20190156>.
31. Al Mamun, M.A.; Asim, M.M.H.; Sahin, M.A.Z.; Al-Bari, M.A.A. Flavonoids compounds from *Tridax procumbens* inhibit osteoclast differentiation by down-regulating c-Fos activation. *J Cell Mol Med.* **2020**, *24*, 2542-2551, <https://doi.org/10.1111/jcmm.14948>.
32. Grace, V.B.; Viswanathan, S.; Wilson, D.D.; Kumar, S.J.; Sahana, K.; Arbin, E.M.; Narayanan, J. Significant action of *Tridax procumbens* L. leaf extract on reducing the TNF- $\alpha$  and COX-2 gene expressions in induced inflammation site in Swiss albino mice. *Inflammopharmacology* **2019**, *57*, 5480-5485, <https://doi.org/10.1021/jf900420g>.
33. Bhagat, V.C.; Kondawar, M.S. Antitubercular potential of *Dendrophthoe falcate* (L.) and *Tridax procumbens* (L.) Plants extracts against h37rv stain of mycobacteria tuberculosis. *Int J Pharm Sci Res.* **2018**, *10*, 251-259, [https://doi.org/10.13040/IJPSR.0975-8232.10\(1\).251-59](https://doi.org/10.13040/IJPSR.0975-8232.10(1).251-59).
34. Manjamalai, A.; Kumar, M.J.; Grace, V.M. Essential oil of *Tridax procumbens* L induces apoptosis and suppresses angiogenesis and lung metastasis of the B16F-10 cell line in C57BL/6 mice. *Asian Pac J Cancer Prev.* **2012**, *13*, 5887-5895, <https://doi.org/10.7314/apjcp.2012.13.11.5887>.
35. Warrier, P.K. *Indian medicinal plants: a compendium of 500 species*. Orient Blackswan, Volume 5, **1993**.
36. Taylor, R.S.L.; Hudson, J.B.; Manandhar, N.P.; Towers, G.H.N. Antiviral activities of medicinal plants of southern Nepal. *J Ethnopharmacol.* **1996**, *53*, 105-110, [https://doi.org/10.1016/S0378-8741\(96\)01430-4](https://doi.org/10.1016/S0378-8741(96)01430-4).
37. Rothan, H.A.; Zulqarnain, M.; Ammar, Y.A.; Tan, E.C.; Rahman, N.A.; Yusof, R. Screening of antiviral activities in medicinal plants extracts against dengue virus using dengue NS2B-NS3 protease assay. *Trop. Biomed.* **2014**, *31*, 286-296.
38. Joshi, R.K.; Badakar, V. Chemical composition and in vitro antimicrobial activity of the essential oil of the flowers of *Tridax procumbens*. *Nat Prod Commun.* **2012**, *7*, <https://doi.org/10.1177/1934578X1200700736>.
39. Oellien, F.; Nicklaus, M.C. Online SMILES translator and structure file generator. *National Cancer Institute* **2004**, *29*, 97-101.
40. Ayers, M. ChemSpider: the free chemical database. *Reference Review* **2012**, *26*, 45-46, <https://doi.org/10.1108/09504121211271059>.
41. Dallakyan, S.; Olson, A.J. Small-molecule library screening by docking with PyRx. *Chemical biology Humana Press, New York, NY* **2015**, *1263*, 243-250, [https://doi.org/10.1007/978-1-4939-2269-7\\_19](https://doi.org/10.1007/978-1-4939-2269-7_19).
42. Trott, O.; Olson, A.J. AutoDock Vina: improving the speed and accuracy of docking with a new scoring function, efficient optimization, and multithreading. *J Comput Chem.* **2010**, *31*, 455-461, <https://doi.org/10.1002/jcc.21334>.
43. Biovia, D.S.; Dsme, R. *San Diego: Dassault Systèmes.* **2015**.
44. Daina, A.; Michielin, O.; Zoete, V. SwissADME: a free web tool to evaluate pharmacokinetics, drug-likeness and medicinal chemistry friendliness of small molecules. *Sci Rep.* **2017**, *7*, <https://doi.org/10.1038/srep42717>.
45. Pires, D. E.; Blundell, T.L.; Ascher, D.B. pkCSM: predicting small-molecule pharmacokinetic and toxicity properties using graph-based signatures. *J Med Chem.* **2015**, *58*, 4066-4072, <https://doi.org/10.1021/acs.jmedchem.5b00104>.
46. Gfeller, D.; Grosdidier, A.; Wirth, M.; Daina, A.; Michielin, O.; Zoete, V. SwissTargetPrediction: a web server for target prediction of bioactive small molecules. *Nucleic Acids Res.* **2014**, *42*, W32-W38, <https://doi.org/10.1186/s12859-017-1586-z>.
47. Lipinski, C.A. Lead-and drug-like compounds: the rule-of-five revolution. *Drug Discov Today Technol.* **2004**, *1*, 337-341, <https://doi.org/10.1016/j.ddtec.2004.11.007>.
48. Qidwai, T. QSAR modelling, docking and ADMET studies for exploration of potential anti-malarial compounds against *Plasmodium falciparum*. *In silico Pharmacol.* **2016**, *5*, <https://doi.org/10.1007/s40203-017-0026-0>.
49. Fonteh, P.; Elkhadir, A.; Omondi, B.; Guzei, I.; Darkwa, J.; Meyer, D. Impedance technology reveals correlations between cytotoxicity and lipophilicity of mono and bimetallic phosphine complexes. *Biometals.* **2015**, *28*, 653-667, <https://doi.org/10.1007/s10534-015-9851-y>.
50. Daina, A.; Michielin, O.; Zoete, V. SwissTargetPrediction: updated data and new features for efficient prediction of protein targets of small molecules. *Nucleic Acids Res.* **2019**, *47*, W357-W364, <https://doi.org/10.1093/nar/gkz382>.
51. Islam, R.; Parves, M.R.; Paul, A.S.; Uddin, N.; Rahman, M.S.; Mamun, A.A.; Hossain, M.N.; Ali, M.A.; Halim, M.A. A molecular modeling approach to identify effective antiviral phytochemicals against the main protease of SARS-CoV-2. *J Biomol Struct Dyn.* **2020**, 1-12, <https://doi.org/10.1080/07391102.2020.1761883>.

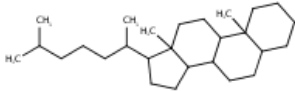
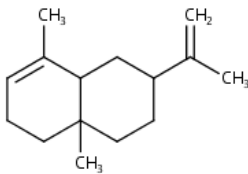
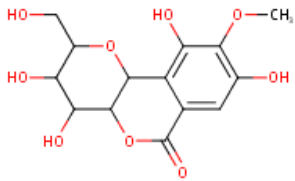
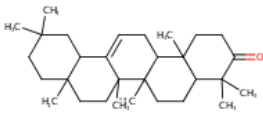
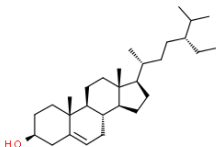
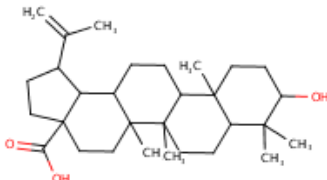
52. Talele, T.T.; Khedkar, S.A.; Rigby, A.C. Successful applications of computer aided drug discovery: moving drugs from concept to the clinic. *Curr Top Med Chem.* **2010**, *10*, 127-141, <https://doi.org/10.2174/156802610790232251>.
53. Enmozhi, S.K.; Raja, K.; Sebastine, I.; Joseph, J. Andrographolide as a potential inhibitor of SARS-CoV-2 main protease: an *in silico* approach. *J Biomol Struct Dyn.* **2020**, 1-7, <https://doi.org/10.1080/07391102.2020.1760136>.
54. Ponnulakshmi, R.; Shyamaladevi, B.; Vijayalakshmi, P.; Selvaraj, J. *In silico* and *in vivo* analysis to identify the antidiabetic activity of beta sitosterol in adipose tissue of high fat diet and sucrose induced type-2 diabetic experimental rats. *Toxicol Mech Methods* **2019**, *29*, 276-290, <https://doi.org/10.1080/15376516.2018.1545815>.
55. Rathod, J.D.; Pathak, N.L.; Patel, R.G.; Jivani, N.P.; Bhatt N.M. Phytopharmacological properties of *Bambusa arundinacea* as a potential medicinal tree: an Overview. *J. Appl. Pharm. Sci.* **2011**, *1*, 27-31.
56. Huang, Y F.; Bai, C.; He, F.; Xie, Y.; Zhou, H. Review on the potential action mechanisms of Chinese medicines in treating Coronavirus Disease 2019 (COVID-19). *Pharmacol. Res. Commun.* **2020**, *158*, 1043-6618, <https://doi.org/10.1016/j.phrs.2020.104939>.
57. Towler, P.; Staker, B.; Prasad, S.G. ACE2 X-ray structures reveal a large hinge-bending motion important for inhibitor binding and catalysis. *J Biol Chem.* **2004**, *279*, 17996-18007, <https://doi.org/10.1074/jbc.M311191200>.
58. Gao, Y.; Yan, L.; Huang, Y.; Liu, F.; Zhao, Y.; Cao, L.; Wang, T.; Sun, Q.; Ming, Z.; Zhang, L.; GE, J.; Zheng, L.; Zhang, Y.; Wang, H.; Zhu, Y.; Zhu, C.; Hu, T.; Hua, T.; Zhang, B.; Yang, X.; Li, J.; Yang, H.; Liu, Z.; Xu, W.; Guddat, W.L.; Wang, Q.; Lou, Z.; Rao. The structure of the COVID-19 virus polymerase essential for viral replication provides a basis for the design of new antiviral drugs. *Science* **2020**, *368*, 0779-782.
59. Aftab, S.O.; Ghouri, M.Z.; Masood, M.U.; Haider, Z.; Khan, Z.; Ahmad, A.; Munawar, N. Analysis of SARS-CoV-2 RNA-dependent RNA polymerase as a potential therapeutic drug target using a computational approach. *J Transl Med.* **2020**, *18*, <https://doi.org/10.1186/s12967-020-02439-0>
60. Ding, J.; Das, K.; Hsiou, Y.; Sarafianos, S. G.; Clark, A. D.; Jr, Jacobo-Molina, A.; Tantillo, C.; Hughes, S. H.; Arnold, E. Structure and functional implications of the polymerase active site region in a complex of HIV-1 RT with a double-stranded DNA template-primer and an antibody Fab fragment at 2.8 Å resolution. *J Mol Biol.* **1998**, *284*, 1095-1111, <https://doi.org/10.1006/jmbi.1998.2208>.
61. Huang, H.; Chopra, R.; Verdine, L.G.; Harrison, C.S. Structure of a Covalently Trapped Catalytic Complex of HIV-1 Reverse Transcriptase: Implications for Drug Resistance. *Science* **1998**, *282*, 1669-1675, <https://doi.org/10.1126/science.282.5394.1669>.
62. Hu, W.S.; Hughes, S.H. HIV-1 reverse transcription. *Cold Spring Harb Perspect Med.* **2012**, *2*, <https://doi.org/10.1101/cshperspect.a006882>.
63. Shu, Q.; Lennemann, N.J.; Sarkar, S.N.; Sadovsky, Y.; Coyne, C.B. ADAP2 Is an Interferon Stimulated Gene That Restricts RNA Virus Entry. *PLoS Pathog.* **2015**, *11*, <https://doi.org/10.1371/journal.ppat.1005150>.
64. Jin, Z.; Du, X.; Xu, Y. Structure of Mpro from SARS-CoV-2 and discovery of its inhibitors. *Nature* **2020**, *582*, 289-293, <https://doi.org/10.1038/s41586-020-2223-y>.
65. Zhang, L.; Lin, D.; Sun, X.; Curth, U.; Drosten, C.; Sauerhering, L.; Becker, S.; Rox, K.; Hilgenfeld, R. Crystal structure of SARS-CoV-2 main protease provides a basis for design of improved  $\alpha$ -ketoamide inhibitors. *Science* **2020**, *368*, 409-412, <https://doi.org/10.1126/science.abb3405>.
66. Zhang, T.; Chen, D. Anticomplementary principles of a Chinese multiherb remedy for the treatment and prevention of SARS. *J Ethnopharmacol.* **2008**, *117*, 351-361, <https://doi.org/10.1016/j.jep.2008.02.012>.
67. Theoharides T. C. COVID-19, pulmonary mast cells, cytokine storms, and beneficial actions of luteolin. *Biofactors* **2020**, *46*, 306-308, <https://doi.org/10.1002/biof.1633>.
68. Ryu, Y.B.; Jeong, H.J.; Kim, J.H.; Kim, Y.M.; Park, J.Y., Kim, D., Nguyen, T.T., Park, S.J., Chang, J.S.; Park, K.H., Rho, M.C.; Lee, W.S. Biflavonoids from *Torreya nucifera* displaying SARS-CoV 3CL(pro) inhibition. *Bioorg. Med. Chem.* **2010**, *18*, 7940-7947, <https://doi.org/10.1016/j.bmc.2010.09.035>.
69. Belouzard, S.; Millet, J.K.; Licitra, B.N.; Whittaker, G.R. Mechanisms of coronavirus cell entry mediated by the viral spike protein. *Viruses* **2012**, *4*, 1011-1033, <https://doi.org/10.3390/v4061011>.
70. Gómara, M.J.; Mora, P.; Mingarro, I.; Nieva, J.L. Roles of a conserved proline in the internal fusion peptide of Ebola glycoprotein. *FEBS let.* **2004**, *569*, 261-266, <https://doi.org/10.1016/j.febslet.2004.06.006>.
71. Luo, Z.; Matthews, A.M.; Weiss, S.R. Amino acid substitutions within the leucine zipper domain of the murine coronavirus spike protein cause defects in oligomerization and the ability to induce cell-to-cell fusion. *J Virol.* **1999**, *73*, 8152-8159, <https://doi.org/10.1128/JVI.73.10.8152-8159.1999>.
72. Prinsloo, G.; Marokane, C.K.; Street, R.A. Anti-HIV activity of southern African plants: Current developments, phytochemistry and future research. *J Ethnopharmacol.* **2018**, *210*, 133-155, <https://doi.org/10.1016/j.jep.2017.08.005>.
73. Rajbhandari, M.; Mentel, R.; Jha, P. K.; Chaudhary, R.P.; Bhattarai, S.; Gewali, M.B.; Karmacharya, N.; Hipper, M.; Lindequist, U. Antiviral activity of some plants used in Nepalese traditional medicine. *Evid Based Complement Alternat Med.* **2009**, *6*, 517-522, <https://doi.org/10.1093/ecam/nem156>.

74. Rai, V.; Kumar, A.; Das, V.; Ghosh, S. Evaluation of chemical constituents and in vitro antimicrobial, antioxidant and cytotoxicity potential of rhizome of *Astilberivularis* (Bodho-okhati), an indigenous medicinal plant from Eastern Himalayan region of India. *BMC Complement Altern Med.* **2019**, *19*, <https://doi.org/10.1186/s12906-019-2621-6>.
75. Abbasifard, M.; Khorramdelazad, H. The bio-mission of interleukin-6 in the pathogenesis of COVID-19: A brief look at potential therapeutic tactics. *Life Sci.* **2020**, *257*, <https://doi.org/10.1016/j.lfs.2020.118097>.
76. Walls, A.C.; Park, Y.J.; Tortorici, M.A.; Wall, A.; McGuire, A.T.; Veesler, D. Structure, Function, and Antigenicity of the SARS-CoV-2 Spike Glycoprotein. *Cell* **2020**, *181*, 281-292; <https://doi.org/10.1016/j.cell.2020.02.058>.
77. Xing, Z.H.; Ma, Y.C.; Li, X.P.; Zhang, B.; Zhang, M.D. Zhongguo Zhong yao za zhi = Zhongguozhongyaozazhi. *China journal of Chinese materia medica* **2017**, *42*, 3703-3708, <https://doi.org/10.19540/j.cnki.cjcmm.20170907.003>.
78. Fang, M.; Liu, S.; Wang, Q.; Gu, X.; Ding, P.; Wang, W.; Ding, Y.; Liu, J.; Wang, R. Qualitative and Quantitative Analysis of 24 Components in Jinlianhua Decoction by UPLC-MS/MS. *Chromatographia* **2019**, *82*, 1801-1825, <https://doi.org/10.1007/s10337-019-03806-w>.
79. Ojo, O.A.; Ojo, A.B.; Taiwo, O.A.; Oluba, O.M. Novel Coronavirus (SARS-CoV-2) Main Protease: Molecular docking of Puerarin as a Potential inhibitor. *Research Article* **2020**, <https://doi.org/10.21203/rs.3.rs-37794/v1>.
80. Ashkenazy, H.; Abadi, S.; Martz, E.; Chay, O.; Mayrose, I.; Pupko, T.; Ben-Tal, N. ConSurf 2016: an improved methodology to estimate and visualize evolutionary conservation in macromolecules. *Nucleic Acids Res.* **2016**, *44*, W344-W350, <https://doi.org/10.1093/nar/gkw408>.
81. Poch, O.; Sauvaget, I.; Delarue, M.; Tordo, N. Identification of four conserved motifs among the RNA-dependent polymerase encoding elements. *EMBO J.* **1989**, *8*, 3867-3874.
82. Kirchdoerfer, R.N.; Ward, A.B. Structure of the SARS-CoV nsp12 polymerase bound to nsp7 and nsp8 co-factors. *Nat. Commun.* **2019**, *10*, <https://doi.org/10.1038/s41467-019-10280-3>.
83. Chang, S.L.; Chiang, Y.M.; Chang, C.L.T.; Yeh, H.H.; Shyur, L.F.; Kuo, Y.H.; Wu, T.K.; Yang, W.C. Flavonoids, centaurein and centaureidin, from *Bidens pilosa*, stimulate IFN- $\gamma$  expression. *J Ethnopharmacol.* **2007**, *112*, 232-236, <https://doi.org/10.1016/j.jep.2007.03.001>.
84. Seelinger, G.; Merfort, I.; Schempp, C.M. Anti-oxidant, anti-inflammatory and anti-allergic activities of luteolin. *Planta Med.* **2008**, *74*, 1667-1677, <https://doi.org/10.1055/s-0028-1088314>.
85. Potočnjak, I.; Šimić, L.; Gobin, I.; Vukelić, I.; Domitrović, R. Antitumor activity of luteolin in human colon cancer SW620 cells is mediated by the ERK/FOXO3a signaling pathway. *Toxicol in Vitro.* **2020**, *66*, <https://doi.org/10.1016/j.tiv.2020.104852>.
86. Liang, J.; Li, Y.; Liu, X.; Huang, Y.; Shen, Y.A.N.; Wang, J.U.N.; Liu, Z.; Zhao, Y.A. In vivo and in vitro anti-malarial activity of bergenin. *Biomed Rep.* **2014**, *2*, 260-264, <https://doi.org/10.3892/br.2013.207>.
87. Patel, D.K.; Patel, K.; Kumar, R.; Gadewar, M.; Tahilyani, V. Pharmacological and analytical aspects of bergenin: a concise report. *Asian Pac J Trop Dis.* **2012**, *2*, 163-167, [https://doi.org/10.1016/S2222-1808\(12\)60037-1](https://doi.org/10.1016/S2222-1808(12)60037-1).
88. Patel, R.; Vanzara, A.; Patel, N.; Vasava, A.; Patil, S.; Rajput, K. Discovery of fungal metabolites bergenin, quercitrin and dihydroartemisinin as potential inhibitors against main protease of SARS-CoV-2. *Preprint: ChemRxiv* **2020**, <https://doi.org/10.26434/chemrxiv.12523136.v1>.
89. Ribeiro, D.; Freitas, M.; Lima, J.L.; Fernandes, E. Proinflammatory pathways: the modulation by flavonoids. *Med Res Rev.* **2015**, *35*, 877-936, <https://doi.org/10.1002/med.21347>.
90. Mada, S.R.; Metukuri, M.R.; Burugula, L.; Reddanna, P.; Krishna, D.R. Antiinflammatory and antinociceptive activities of gossypin and procumbentin-cyclooxygenase-2 (COX-2) inhibition studies. *Phytother Res.* **2009**, *23*, 878-884, <https://doi.org/10.1002/ptr.2727>.

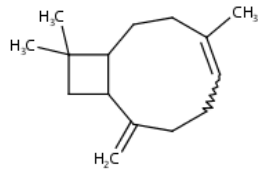
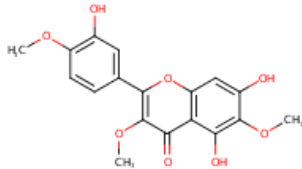
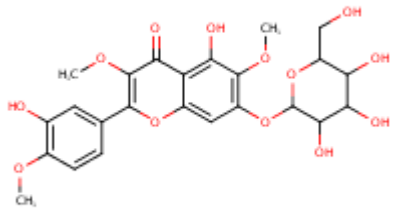
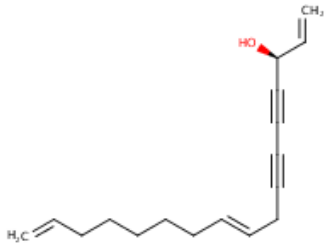
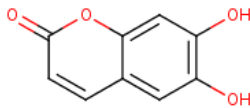
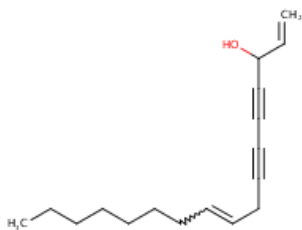


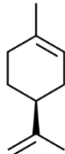
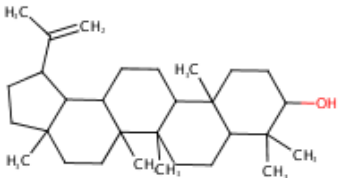
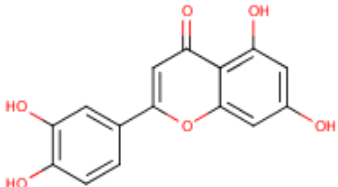
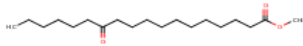
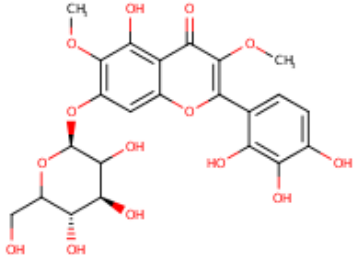
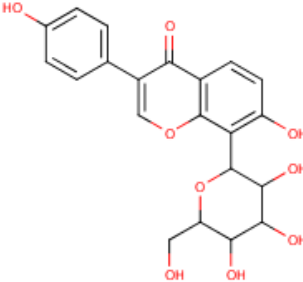
## Supplementary Data

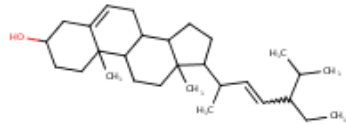
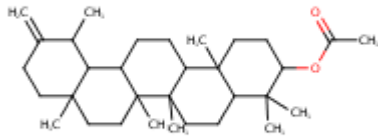
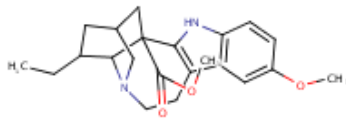
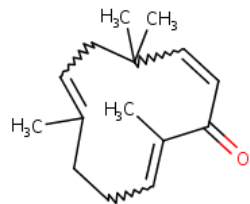
**Table S1.** Ingredients of *Tridax procumbens* used for *in silico* screening against various proteins of SARS-CoV-2.

Sr.No	Name of Compound	Molecular Formula	PubChem CID:	Structure
01	5(alpha)-cholestane	C <sub>27</sub> H <sub>48</sub>	10202	
02	alpha-Selinene	C <sub>15</sub> H <sub>24</sub>	10856614	
03	Bergenin	C <sub>14</sub> H <sub>16</sub> O <sub>9</sub>	66065	
04	beta-Amyrenone	C <sub>30</sub> H <sub>48</sub> O	12306160	
05	beta-Sitosterol	C <sub>29</sub> H <sub>50</sub> O	222284	
06	Betulinic acid	C <sub>30</sub> H <sub>48</sub> O <sub>3</sub>	64971	



Sr.No	Name of Compound	Molecular Formula	PubChem CID:	Structure
07	Caryophyllene	$C_{15}H_{24}$	5281515	
08	Centaureidin	$C_{18}H_{16}O_8$	5315773	
09	Centaurein	$C_{24}H_{26}O_{13}$	5489090	
10	(3,S)-16,17-Didehydrofalcarinol	$C_{17}H_{22}O$	6442009	
11	Esculetin	$C_9H_6O_4$	5281416	
12	Falcarinol	$C_{17}H_{24}O$	5281149	

Sr.No	Name of Compound	Molecular Formula	PubChem CID:	Structure
13	Limonene	C <sub>10</sub> H <sub>16</sub>	22311	
14	Lupeol	C <sub>30</sub> H <sub>50</sub> O	259846	
15	Luteolin	C <sub>15</sub> H <sub>10</sub> O <sub>6</sub>	5280445	
16	Methyl 10-oxooctadecanoate	C <sub>19</sub> H <sub>36</sub> O <sub>3</sub>	543603	
17	Procumbentin	C <sub>23</sub> H <sub>24</sub> O <sub>14</sub>	-	
18	Puerarin	C <sub>21</sub> H <sub>20</sub> O <sub>9</sub>	5281807	

Sr.No	Name of Compound	Molecular Formula	PubChem CID:	Structure
19	Stigmasterol	$C_{29}H_{48}O$	5280794	
20	Taraxasterol acetate	$C_{32}H_{52}O_2$	13889352	
21	Voacangine	$C_{22}H_{28}N_2O_3$	73255	
22	Zerumbone	$C_{15}H_{22}O$	5470187	

**Table S2.** Physiochemical and ADMET properties of Ingredients of *Tridax procumbens* (using SwissADME).

Sr. No.	Name of Compound	Molecular weight (g/mol)	cLogP	cLogS	HBA	HBD	TSA (Å²)	GI absorption	BBB Permeability	Skin Permeation (cm/s)
01	5(alpha)- cholestane	372.67	5.16	-8.80	0	0	0.00	Low	No	-0.71
02	alpha-Selinene	204.35	3.31	-4.95	0	0	0.00	Low	No	-3.85
03	Bergenin	328.27	1.55	-1.61	9	5	145.91	Low	No	-8.99
04	beta-Amyrenone	424.70	4.53	-9.08	1	0	17.07	Low	No	-2.61
05	beta-Sitosterol	414.71	4.79	-9.67	1	1	20.23	Low	No	-2.20
06	Betulinic acid	456.70	3.68	-9.28	3	2	57.53	Low	No	-3.26
07	Caryophyllene	204.35	3.29	-3.87	0	0	0.00	Low	No	-4.44
08	Centaureidin	360.31	2.98	-4.94	8	3	118.59	High	No	-6.52
09	Centaurein	522.46	2.53	-4.73	13	6	197.74	Low	No	-8.78
10	(3,S)-16,17-Didehydrofalcarinol	242.36	4.00	-5.13	1	1	20.23	High	Yes	-4.25
11	Esculetin	178.14	1.25	-2.30	4	2	70.67	High	No	-6.52
12	Falcarinol	244.37	3.86	-4.29	1	1	20.23	High	Yes	3.89
13	Limonene	136.23	2.72	-4.29	0	0	0.00	Low	Yes	-3.89
14	Lupeol	426.72	4.89	-10.22	1	1	20.23	Low	No	-1.90
15	Luteolin	286.24	1.86	-4.51	6	4	111.13	High	No	-6.25
16	Methyl 10-oxooctadecanoate	312.49	4.37	-4.65	3	0	43.37	High	Yes	-3.70
17	Procumbentin	524.43	2.37	-3.20	14	8	228.97	Low	No	-9.29
18	Puerarin	416.38	1.96	-2.94	9	6	160.82	Low	No	-8.83
19	Stigmasterol	412.69	4.96	-7.46	1	1	20.23	Low	No	-2.74
20	Taraxasterol acetate	468.75	5.18	-10.17	2	0	26.30	Low	No	-2.27
21	Voacangine	368.47	3.63	-4.34	4	1	54.56	High	Yes	-6.06
22	Zerumbone	218.33	2.72	-3.68	1	0	17.07	High	Yes	-4.83

cLogP -Consensus Log Po/w (Average of all five predictions); cLogS-< -4= Soluble\*HA- Hydrogen Bond Acceptor; HBD: Hydrogen Bond Donor; TSA- Topological Polar Surface Area:

**Table S3.** Physiochemical and ADMET properties of Ingredients of *Tridaxprocumbens* -Predicted lead likeness, Drug likeness, and synthetic accessibility score (using SwissADME).

Sr. No.	Name of Compound	Lipinski rule of five*	Ghose filters*	Veber (GSK) filter*	Egan filters*	Muegge (Bayer) filter*	Lead likeness	Synthetic accessibility
01	5(alpha)-cholestane	Yes; 1 violation: MLOGP>4.15	No; 2 violations: WLOGP>5.6, #atoms>70	Yes	No; 1 violation: WLOGP>5.88	No; 2 violations: XLOGP3>5, Heteroatoms<2	No; 2 violations: MW>350, XLOGP3>3.5	5.20
02	alpha-Selinene	Yes; 1 violation: MLOGP>4.15	Yes	Yes	Yes	No; 2 violations: XLOGP3>5, Heteroatoms<2	No; 2 violations: MW<250, XLOGP3>3.5	4.22
03	Bergenin	Yes	No; 1 violation: WLOGP<-0.4	No; 1 violation: TPSA>140	No; 1 violation: TPSA>131.6	Yes	Yes	4.39
04	beta-Amyrenone	Yes; 1 violation: MLOGP>4.15	No; 3 violations: WLOGP>5.6, MR>130, #atoms>70	Yes	No; 1 violation: WLOGP>5.88	No; 2 violations: XLOGP3>5, Heteroatoms<2	No; 2 violations: MW>350, XLOGP3>3.5	5.90
05	beta-Sitosterol	Yes; 1 violation: MLOGP>4.15	No; 3 violations: WLOGP>5.6, MR>130, #atoms>70	Yes	No; 1 violation: WLOGP>5.88	No; 2 violations: XLOGP3>5, Heteroatoms<2	No; 2 violations: MW>350, XLOGP3>3.5	6.30
06	Betulinic acid	Yes; 1 violation: MLOGP>4.15	No; 3 violations: WLOGP>5.6, MR>130, #atoms>70	Yes	No; 3 violations: WLOGP>5.6, MR>130, #atoms>70	No; 1 violation: XLOGP3>5	No; 2 violations: MW>350, XLOGP3>3.5	5.63
07	Caryophyllene	Yes; 1 violation: MLOGP>4.15	Yes	Yes	Yes	No; 1 violation: Heteroatoms<2	No; 2 violations: MW<250, XLOGP3>3.5	4.51
08	Centaureidin	Yes	Yes	Yes	Yes	Yes	No; 1 violation: MW>350	3.57
09	Centaurein	No; 3 violations: MW>500, NorO>10, NHorOH>5	No; 1 violation: MW>480	No; 1 violation: TPSA>140	No; 1 violation: TPSA>131.6	No; 3 violations: TPSA>150, Hacc>10, H-don>5	No; 1 violation: MW>350	5.70
10	(3,S)-16,17-Didehydrofalcarninol	No; 1 violation: Heteroatoms<2	Yes	Yes	Yes	No; 1 violation: Heteroatoms<2	No; 3 violations: MW<250, Rotors>7, XLOGP3>3.5	4.26
11	Esculetin	Yes	No; 1 violation: #atoms<20	Yes	Yes	No; 1 violation: MW<200	No; 1 violation: MW<250	2.61
12	Falcarninol	Yes; 1 violation: MLOGP>4.15	Yes	Yes	Yes	No; 2 violations: XLOGP3>5, Heteroatoms<2	No; 3 violations: MW<250, Rotors>7, XLOGP3>3.5	4.33
13	Limonene	Yes	No; 1 violation: MW<160	Yes	Yes	No; 2 violations: MW<200, Heteroatoms<2	No; 2 violations: MW<250, XLOGP3>3.5	3.46



14	Lupeol	Yes; 1 violation: MLOGP>4.15	No; 3 violations: WLOGP>5.6, MR>130, #atoms>70	Yes	No; 1 violation: WLOGP>5.88	No; 2 violations: XLOGP3>5, Heteroatoms<2	No; 2 violations: MW>350, XLOGP3>3.5	5.49
15	Luteolin	Yes	Yes	Yes	Yes	Yes	Yes	3.02
16	Methyl 10-oxooctadecanoate	Yes	Yes	No; 1 violation: Rotors>10	Yes	No; 2 violations: XLOGP3>5, Rotors>15	No; 2 violations: Rotors>7, XLOGP3>3.5	2.73
17	Procumbentin	No; 3 violations: MW>500, NorO>10, NHorOH>5	No; 2 violations: MW>480, WLOGP<-0.4	No; 1 violation: TPSA>140	No; 1 violation: TPSA>131.6	No; 3 violations: TPSA>150, H-acc>10, H-don>5	No; 1 violation: MW>350	5.69
18	Puerarin	Yes; 1 violation: NHorOH>5	Yes	No; 1 violation: TPSA>140	No; 1 violation: TPSA>131.6	No; 2 violations: TPSA>150, H-don>5	No; 1 violation: MW>350	4.98
19	Stigmasterol	Yes; 1 violation: MLOGP>4.15	No; 3 violations: WLOGP>5.6, MR>130, #atoms>70	Yes	No; 1 violation: WLOGP>5.88	No; 2 violations: XLOGP3>5, Heteroatoms<2	No; 2 violations: MW>350, XLOGP3>3.5	6.21
20	Taraxasterol acetate	Yes; 1 violation: MLOGP>4.15	No; 3 violations: WLOGP>5.6, MR>130, #atoms>70	Yes	No; 1 violation: WLOGP>5.88	No; 1 violation: XLOGP3>5	No; 2 violations: MW>350, XLOGP3>3.5	5.61
21	Voacangine	Yes	Yes	Yes	Yes	Yes	No; 2 violations: MW>350, XLOGP3>3.5	4.88
22	Zerumbone	Yes	Yes	Yes	Yes	No; 1 violation: Heteroatoms<2	No; 2 violations: MW<250, XLOGP3>3.5	3.47

\*Applied Lipinski rule of five- Ghose, Veber, Egan, and Muegge rules;  
Synthetic accessibility range (0-10) = very easy to very difficult to synthesize

**Table S4.** Pharmacokinetic Properties- Predicted ADMET properties of Ingredients of *Tridax procumbens* (using pkCSM).

Absorption Property								
Sr. No.	Name of Compound	Water solubility (log mol/L)	Caco2 permeability (log Papp in 10 <sup>-6</sup> cm/s)	Intestinal absorption (human) (% Absorbed)	Skin Permeability (log Kp)	P-gp substrate	P-gp I inhibitor	P-gp II inhibitor
01	5(alpha)- cholestane	-5.619	1.263	97.135	-2.724	No	No	Yes
02	alpha-selinene	-6.074	1.401	94.127	-1.461	No	No	No
03	Bergenin	-1.853	0.289	63.774	-2.736	Yes	No	No
04	beta-Amyrenone	-6.741	1.332	96.254	-2.733	No	Yes	Yes
05	beta-Sitosterol	-6.773	1.201	94.464	-2.783	No	Yes	Yes
06	Betulinic acid	-3.122	1.175	99.763	-2.735	No	No	No
07	Caryophyllene	-5.555	1.423	94.845	-1.58	No	No	No
08	Centaureidin	-3.221	0.161	77.207	-2.735	Yes	No	Yes
09	Centaurein	-2.995	0.294	35.872	-2.735	Yes	No	No
10	(3,S)-16,17-Didehydrofalcarinol	-5.712	1.513	94.685	-2.028	No	No	No
11	Esculetin	-2.497	0.301	86.291	-2.796	Yes	No	No
12	Falcarinol	-5.84	1.513	94.209	-2.028	No	No	No
13	Limonene	-3.568	1.401	95.898	-1.721	Yes	No	No
14	Lupeol	-5.861	1.226	95.782	-2.744	No	Yes	Yes
15	Luteolin	-3.094	0.096	81.13	-2.735	Yes	No	No
16	Methyl 10-oxooctadecanoate	-5.946	1.614	93.432	-2.712	No	Yes	No
17	Procumbentin	-2.918	-1.418	31.97	-2.735	Yes	No	No
18	Puerarin	-2.72	0.223	67.446	-2.735	Yes	No	No
19	Stigmasterol	-6.682	1.213	94.97	-2.783	No	Yes	Yes
20	Taraxasterol acetate	-5.804	1.218	98.464	-2.737	No	Yes	Yes
21	Voacangine	-3.427	1.108	93.462	-2.905	Yes	Yes	No
22	Zerumbone	-4.027	1.432	95.781	-2.06	No	No	No

\*P-gp- P -glycoprotein

### Distribution Property

Sr. No.	Name of Compound	VDss (human) (log L/kg)	Fraction unbound (human) (Fu)	BBB permeability (log BB)	CNS permeability (log PS)
01	5(alpha)- cholestane	-0.148	0.012	1	-0.648
02	aplha-selinene	0.686	0.186	0.776	-1.865
03	Bergenin	0.68	0.632	-1.091	-3.903
04	beta-Amyrenone	0.246	0	0.694	-1.747
05	beta-Sitosterol	0.193	0	0.781	-1.705
06	Betulinic acid	-1.18	0.018	-0.322	-1.343
07	Caryophyllene	0.652	0.263	0.733	-2.172
08	Centaureidin	0.098	0.067	-1.466	-3.256
09	Centaurein	0.211	0.114	-1.976	-4.267
10	(3,S)-16,17-Didehydrofalcarinol	0.308	0.137	0.775	-1.467
11	Esculetin	0.528	0.484	0.025	-2.296
12	Falcarinol	0.313	0.127	0.765	-1.467
13	Limonene	0.396	0.48	0.732	-2.37
14	Lupeol	0	0	0.726	-1.714
15	Luteolin	1.153	0.168	-0.907	-2.251
16	Methyl 10-oxooctadecanoate	0.041	0.056	-0.226	-1.834
17	Procumbentin	1.132	0.143	-2.407	-4.826
18	Puerarin	0.377	0.187	-1.204	-3.594
19	Stigmasterol	0.178	0	0.771	-1.652
20	Taraxasterol acetate	-0.165	0	0.622	-1.708
21	Voacangine	1.321	0.296	-0.051	-2.193
22	Zerumbone	0.279	0.395	0.522	-2.647

### Metabolism Property

Sr. No.	Name of Compound	(log ml/min/kg)	CYP3A4 substrate	CYP1A2 inhibitor	CYP2C19 inhibitor	CYP2C9 inhibitor	CYP2D6 inhibitor	CYP3A4 inhibitor
01	5(alpha)- cholestane	No	Yes	No	No	No	No	No
02	alpha-selinene	No	Yes	No	No	No	No	No
03	Bergenin	No	No	No	No	No	No	No
04	beta-Amyrenone	No	Yes	No	No	No	No	No
05	beta-Sitosterol	No	Yes	No	No	No	No	No
06	Betulinic acid	No	Yes	No	No	No	No	No
07	Caryophyllene	No	No	No	No	No	No	No
08	Centaureidin	No	No	Yes	No	No	No	No
09	Centaurein	No	No	No	No	No	No	No
10	(3,S)-16,17-Didehydrofalcarinol	No	Yes	Yes	No	No	No	No
11	Esculetin	No	No	Yes	No	No	No	No
12	Falcarinol	No	Yes	Yes	No	No	No	No
13	Limonene	No	No	No	No	No	No	No
14	Lupeol	No	Yes	No	No	No	No	No
15	Luteolin	No	No	Yes	No	Yes	No	No
16	Methyl 10-oxooctadecanoate	No	Yes	Yes	No	No	No	No
17	Procumbentin	No	No	No	No	No	No	No
18	Puerarin	No	No	No	No	No	No	No
19	Stigmasterol	No	Yes	No	No	No	No	No
20	Taraxasterol acetate	No	Yes	No	No	No	No	No
21	Voacangine	Yes	Yes	No	No	No	Yes	No
22	Zerumbone	No	No	No	No	No	No	No

### Excretion Property

Sr. No.	Name of Compound	Total Clearance (log ml/min/kg)	Renal OCT2 substrate
01	5(alpha)- cholestane	0.57	No
02	aplha-selinene	1.172	No
03	Bergenin	0.427	No
04	beta-Amyrenone	-0.096	No
05	beta-Sitosterol	0.628	No
06	Betulinic acid	0.116	No
07	Caryophyllene	1.088	No
08	Centaureidin	0.562	No
09	Centaurein	0.536	No
10	(3,S)-16,17-Didehydrofalcarinol	2.038	No
11	Esculetin	0.671	No
12	Falcarinol	1.952	No
13	Limonene	0.213	No
14	Lupeol	0.153	No
15	Luteolin	0.495	No
16	Methyl 10-oxooctadecanoate	1.971	No
17	Procumbentin	0.429	No
18	Puerarin	-0.007	No
19	Stigmasterol	0.618	No
20	Taraxasterol acetate	0.057	No
21	Voacangine	1.064	Yes
22	Zerumbone	1.314	No



**Toxicity Property**

Sr. No.	Name of Compound	AMES toxicity	MTD <sup>@</sup> (log mg/kg/day)	hERG I inhibitor	hERG II inhibitor	ORT* (mol/kg)	ORCT# (log mg/kg_bw/day)	HEP \$	SS^	TPT+ (log ug/L)	Minnow toxicity (log mM)
01	5(alpha)- cholestane	No	-0.358	No	Yes	2.542	1.26	No	No	0.296	-2.617
02	aplha-selinene	No	-0.018	No	No	1.543	1.351	No	Yes	1.623	0.353
03	Bergenin	No	-0.013	No	No	1.879	3.614	No	No	0.285	5.688
04	beta-Amyrenone	No	-0.316	No	Yes	2.18	0.852	No	No	0.389	-1.738
05	beta-Sitosterol	No	-0.621	No	Yes	2.552	0.855	No	No	0.43	-1.802
06	Betulinic acid	No	0.144	No	No	2.256	2.206	Yes	No	0.285	-1.174
07	Caryophyllene	No	0.351	No	No	1.617	1.416	No	Yes	1.401	0.504
08	Centaureidin	No	0.594	No	No	2.286	2.224	No	No	0.319	1.86
09	Centaurein	No	0.56	No	Yes	2.565	3.805	No	No	0.285	6.387
10	(3,S)-16,17-Didehydrofalcarinol	No	-0.284	No	No	1.287	1.098	No	Yes	2.286	-0.102
11	Esculetin	No	-0.262	No	No	2.337	1.504	No	No	0.39	2.341
12	Falcarinol	No	-0.279	No	No	1.326	1.116	No	Yes	2.291	-0.181
13	Limonene	No	0.777	No	No	1.88	2.336	No	Yes	0.579	1.203
14	Lupeol	No	-0.502	No	Yes	2.563	0.89	No	No	0.316	-1.696
15	Luteolin	No	0.499	No	No	2.455	2.409	No	No	0.326	3.169
16	Methyl 10-oxooctadecanoate	No	0.288	No	No	1.547	2.757	No	Yes	1.638	-1.195
17	Procumbentin	No	0.531	No	Yes	2.574	4.089	No	No	0.285	7.199
18	Puerarin	No	0.642	No	Yes	2.641	4.85	No	No	0.285	4.188
19	Stigmasterol	No	-0.664	No	Yes	2.54	0.872	No	No	0.433	-1.675
20	Taraxasterol acetate	No	-0.465	No	Yes	2.568	2.112	No	No	0.303	-2.031
21	Voacangine	Yes	-0.598	No	Yes	3.161	0.616	No	No	0.414	-0.413
22	Zerumbone	No	1.314	No	No	0.534	No	No	Yes	1.385	1.033

<sup>@</sup>MTD-Max. tolerated dose (human); \*ORT-Oral Rat Acute Toxicity (LD50) ; #ORCT- Oral Rat Chronic Toxicity (LOAEL) ; \$HEP-Hepatotoxicity;

^SS-Skin Sensitisation; +TPT-T.Pyriformis toxicity